EPTT-2020-0106
EVALUATION OF GEOMETRIC ALTERNATIVES TO PROMOTE MIXING IN A TUBULAR PHOTOBIORREACTOR

Daniela M. Koerich
Lisiane F. Carvalho
Leonardo M. Rosa
University of Blumenau
leorosa@gmail.com

Abstract. *Microalgae are microorganisms capable of produce value-added materials such as biofuels, bioplastics and compounds used in pharmaceutics, cosmetics, and human and animal nutrition. Moreover, microalgae have the ability to fix atmospheric* CO_2 *and treat wastewater. Within the photobioreactor, areas further from the illuminated walls have less light radiation. Therefore, agitation is necessary so that all cells have contact with a sufficient amount of light radiation, and thereby promote photosynthesis. In addition, an efficient mixture between microorganisms and the substrate is also necessary in order for microalgae to consume it, producing materials of interest. In this work, 4 geometric configurations are evaluated in terms of their ability to prevent the segregation of microalgae in a tubular photobioreactor, in addition to the smooth tube: a turbulent vortex promoter in cylindrical shape, a ring baffle, and a helical-shaped static mixer. These systems were evaluated using the Computational Fluid Dynamics (CFD) technique, with which three-dimensional simulations were performed, in a turbulent, transient multiphase regime. The pressure drop promoted by each device inserted in the pipeline was also evaluated, as alternatives that require the imposition of very high pressure to maintain the flow rate can make the process unfeasible. Other evaluation criteria were the swirl number of the flow, the uniformity index of the microalgae concentration, the turbulent kinetic energy, and the shear stress promoted by each photobioreactor configuration. Results showed that, depending on the obstacle used, the mixing between the phases can be enhanced, in terms of the swirl number and the turbulent kinetic energy, without the need for high pressure. However, the shear stress may reach values that can be dangerous to the microalgae growth.*

Keywords: *Mixing, Microalgae, CFD, vortices*

1. INTRODUCTION

Microalgae are microorganisms capable of produce value-added materials such as biofuels, bioplastics and compounds used in pharmaceutics, cosmetics, and in human and animal nutrition. Moreover, microalgae have the ability to fix atmospheric CO_2 and treat wastewater. Microalgae cells work through photosynthesis, which depends on two important factors to occur: light and substrate. Gudin and Chaumont (1991) stated that the algae suspension should not be considered as a simple mineral suspension, but as living cells stressed by the flow. Mitsuhashi *et al.* (1994) observed that the *Spirulin* trichome length is reduced abruptly (from an initial value of 300 μm) when this microalgae is exposed to a flow with shear stress above 0.2 Pa. For shear stresses above 0.4 Pa, *Spirulina* is destructed into peaces of almost 50 μm. Gudin and Chaumont (1991) also noticed that reducing the thickness of culture exposed to light radiance, and fixing the mixing issues, tend to increase the cell concentration. Within the photobioreactor, areas further from the illuminated walls have less light radiation. Therefore, agitation is necessary so that all cells have contact with a sufficient amount of light radiation, and thereby promote photosynthesis. In addition, an efficient mixture between microorganisms and the substrate is also necessary in order for microalgae to consume it, producing materials of interest. In processes in which CO_2 is used as a carbon source, as in systems that adopt bubble columns, the gas injection itself promotes the necessary agitation. In other processes, such as raceways, it is necessary to use other methods to promote mixing between the phases, such as hydraulic or mechanical agitation. Regardless of the promoter approach, it is also interesting to maintain a turbulent regime in order to enhance the mixture between the phases. The turbulent kinetic energy quantifies the amount of fluctuations in the flow in relation to the average velocity, and consequently greater contact between the phases on a sub-mesh scale. With the presence of turbulent vortices in the flow, the contact between adjacent fluid portions is more intense, and consequently the mass transfer rate is higher. However, turbulent flows also require more energy for their maintenance.

Su *et al.* (2010) evaluated the effect of including a cylindrical obstacle inside a photobioreactor, and noticed that it may help to promote a destabilization of the flow, promoting a vertical velocity which helps to achieve the homogeneous mixing of medium needed for microalgae growth. On the other hand, Zhang *et al.* (2013) evaluated numerically the flow

Table 1. Phases properties.

Phase	Density [kg/m^3]	Viscosity [Pa s]	Diameter [m]
Fluid medium	1011	8.9×10^{-4}	–
Microalgae	997	–	9.0×10^{-6}

with and without a helical mixer of varying dimensions. The relief which promoted good relation among the evaluated parameters was then evaluated experimentally inside a smooth tube, which enabled an increase of 37.26% in the biomass production. Gómez-Pérez *et al.* (2017) proposed a twisted tubular photobioreactor geometry, and compared it against other alternatives present in the literature (static mixer and spiral tubular). In the proposed geometry, the light-dark cycles frequency of microalgae was increased.

Rossbach *et al.* (2016) studied the use of ring baffles in a reactor to break the catalyst particles accumulation near the riser wall, breaking the core-annulus profile formation. In the evaluated cases, the turbulent kinetic energy dissipation rate was low, enabling the maintainance of turbulence that can promote better solids dispersion. Terashima *et al.* (2009) defined the uniformity index (UI) as a statistical parameter to be used as a single parameter to characterize mixing in a biodigester. By definition, the UI value is bounded between 0 and 2. A maximum value of 2 is reached when the concentrated tracer exists only in a small volume of the system. This value is reduced to zero when the tracer concentration becomes uniform (Terashima *et al.*, 2009). This indicates the degree of mixing of the phases in each cross section of the photobioreactor. Finally, it is also important to evaluate the pressure drop promoted by each device inserted in the pipeline, as alternatives that require the imposition of very high pressure to maintain the flow rate can make the process unfeasible.

In this work, 4 geometric configurations are evaluated in terms of their ability to prevent the segregation of microalgae in a tubular photobioreactor: in addition to the smooth tube, we considered a turbulent vortex promoter in cylindrical shape, a ring baffle, and a helical-shaped static mixer. These systems were evaluated using the Computational Fluid Dynamics (CFD) technique, which provided a detailed description of the mixing parameters in the turbulent multiphase flow.

2. MATERIALS AND METHODS

The tubular photobioreactors considered in this study were based on an experimental unit installed in the Biochemical Engineering Laboratory (LEB), located at the University of Blumenau. It is composed of transparent, smooth tubes with 21 mm in diameter and 1350 mm length. For the numerical studies, we considered a domain with 1500 mm, further extending the outlet position in the simulation when compared to the experimental setup (Fig. 1a). Obstacles of different shapes were included to evaluate its effect on the multiphase flow: an horizontal bar (Fig. 1b), ring baffle (Fig. 1c, inspired by the study of Rossbach *et al.* (2016)), and helical mixer (Fig. 1d). All geometries were designed using FreeCAD software.

The phases considered were a mixture composed of water and substrate, and *Spirulin sp.* microalgae. Their physical properties are specified in Tab. 1. They enter in the photobioreactor at 0.5 m/s (Gómez-Pérez *et al.*, 2017; Zhang *et al.*, 2013), which corresponds to a Reynolds number of about 10,000. The simplification hypothesis adopted to simulate the photobioreactor were:

- the photosynthesis invariably promotes the production of oxygen, which can lead to the formation of gas bubbles. Its effect on the fluid dynamics was considered negligible;
- the phases are interpenetrable, hence the Eulerian-Eulerian approach was used to model the two-phase flow;
- the *Spirulin sp.* microalgae, which constitutes the dispersed phase, was considered to be spherical;
- the concept of an eddy viscosity may be used to model the turbulent behavior of the flow (Boussinesq hyphothesis).

In the Eulerian-Eulerian approach, the continuity equations are expressed as

$$\frac{\partial}{\partial t}(\alpha_l \rho_l) + \nabla \cdot (\alpha_l \rho_l \mathbf{U_l}) = 0 \tag{1}$$

$$\frac{\partial}{\partial t}(\alpha_p \rho_p) + \nabla \cdot (\alpha_p \rho_p \mathbf{U_p}) = 0 \quad , \tag{2}$$

where α represents the volume fraction of each phase, $\mathbf{U}$ is the phase velocity, ρ the density and μ is the viscosity. The subscripts l and p represents the liquid (water and substrate) and particulate (microalgae) phases.

$$\frac{\partial}{\partial t}\rho_k \mathbf{U_l} + \nabla \cdot (\rho \mathbf{U_l} \mathbf{U_l}) = -\nabla p + \nabla[\mu_l^{eff}(\nabla \mathbf{U_l} + (\nabla \mathbf{U_l})^T)] + \rho \mathbf{g} + \mathbf{F_l} \quad , \tag{3}$$

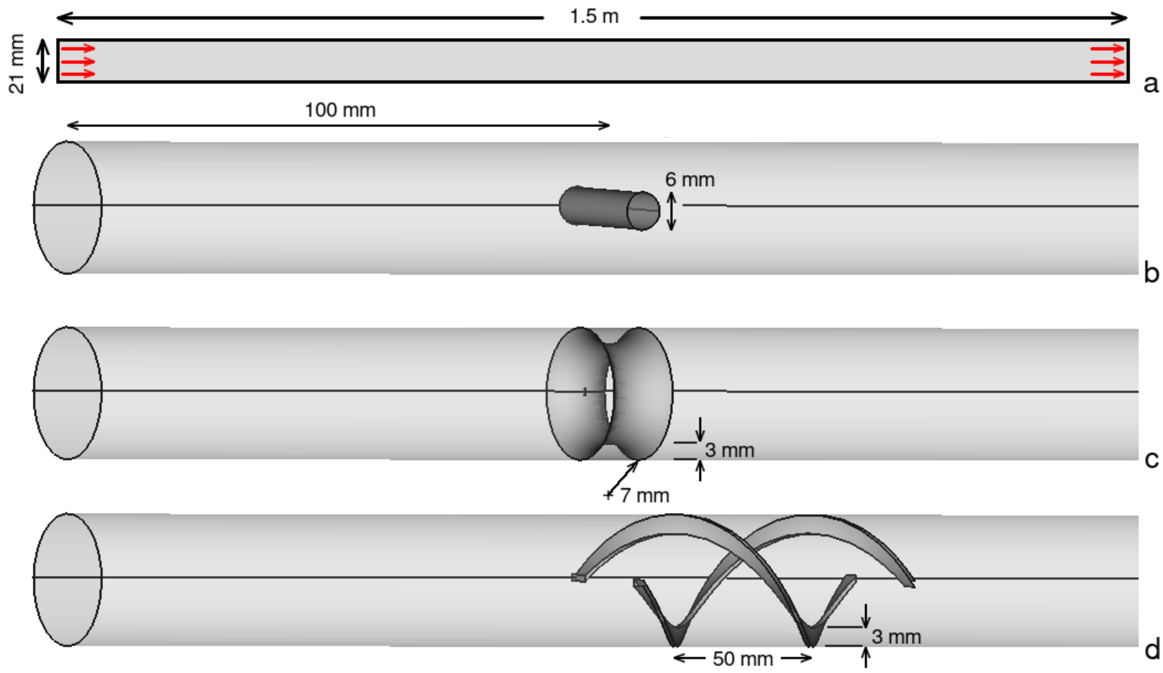

Figure 1. Tubular photobioreactor geometries: (a) smooth tube, (b) horizontal bar, (c) ring baffle, and (d) helical mixer.

$$\frac{\partial}{\partial t}\rho_k \mathbf{U_p} + \nabla \cdot (\rho \mathbf{U_p} \mathbf{U_p}) = -\nabla p + \nabla[\mu_p^{eff}(\nabla \mathbf{U_p} + (\nabla \mathbf{U_p})^T)] + \rho \mathbf{g} + \mathbf{F_p} \quad , \tag{4}$$

where F represents the forces acting on the phases, such as the drag force, and $\mathbf{g}$ is the gravity acceleration.

The drag force was the only interfacial force considered to be acting on the phases. It was modeled using the Gidaspow *et al.* (1983) correlation, which proposes that the drag force in dense regimes ($\alpha_l < 0.8$) may be estimated using an expression based on the Ergun equation. The Ergun model is a function of the phases properties and their relative velocity:

$$M_D = 150\frac{\alpha_p^2 \mu_l}{\alpha_l d_p^2} + 1.75\frac{|\mathbf{U_p} - \mathbf{U_l}|\alpha_p \rho_l}{d_p} \quad , \tag{5}$$

where d_p is the dispersed phase diameter.

For diluted systems, an expression based on the Wen-Yu model is adopted. In this model, the drag force is estimated by:

$$M_D = \frac{3}{4}C_D\frac{|\mathbf{U_p} - \mathbf{U_l}|\alpha_p \rho_l}{d_p} f(\alpha) \quad , \tag{6}$$

where $f(\alpha)$ is defined as:

$$f(\alpha) = \alpha_l^{-2.65} \tag{7}$$

The turbulent behavior of the liquid phase was modeled using the k-ω SST model (Menter, 1994), which was chosen to avoid any deviations in the flow prediction due to the wall functions (Wilcox *et al.*, 1998). In the k-ω SST model, there is one transport equation for the turbulent kinetic energy (k) and another for the specific dissipation rate (ω):

$$\frac{\partial}{\partial t}\rho_l k + \nabla \cdot (U_l k) = \nabla \left[\frac{\mu_l^{eff}}{\sigma_k}\nabla k\right] + G - \rho_l \beta k \omega \quad , \tag{8}$$

$$\frac{\partial}{\partial t}\rho_l \omega + \nabla \cdot (U_l \omega) = \nabla \left[\frac{\mu_l^{eff}}{\sigma_\omega}\nabla \omega\right] + (C_1 G - C_2 \rho_l k \omega)\frac{\omega}{k} + 2(1 - F_1)\sigma_{\omega 2}\frac{\rho}{\omega}\nabla k \cdot \nabla \omega \quad , \tag{9}$$

$$P_k = \min(\tau^{Re} : \nabla \mathbf{v}, c_1 \varepsilon) \tag{10}$$

Using this model, the effective viscosity is obtained with $\mu_l^{eff} = \mu_l + \mu_l^t$, and the turbulent viscosity (μ^t) is calculated by

$$\mu_l^t = \frac{\rho a_1 k}{\max a_1 \omega, \sqrt{2} S_t F_2)} \quad , \tag{11}$$

where C_μ=0.09. The turbulent behavior of the particulate phase was disregarded, hence $\mu_p^{eff} = \mu_p$.

The meshes used to simulate the smooth tube were composed of hexahedral volumes, build using the blockMesh software. Meshes with three sizes were evaluated, and the uncertainty due to the grid refinement was calculated using the GCI method (Roache, 1997). Meshes with 31250, 58500 and 135040 hexahedral control volumes were used. In order to evaluate the uncertainty, predicted values of velocity and volume fraction were collected in 10 points along a vertical line aligned with the Y direction, positioned at the outlet of the fotobioreactor. In addition, in cases considering obstructions, the snappyHexMesh software was used to conform the original mesh to the internal relief.

The turbulent multiphase flow was simulated using a transient formulation with the twoPhaseEulerFoam solver, available in OpenFOAM v7. To carry out the simulations, the Courant number were fixed in 0.9, and the standard relaxation factors (equal to 1) were applied. Cases were simulated for about 5 s of flow, which is higher than the residence time. The calculations were performed in a Dell XPS station with 16 GB RAM and a CPU with 3.6 GHz.

The pressure drop was defined as the difference between the average pressure at the outlet and the inlet of the bioreactor. The value resulting from the flow in the smooth tube was used as a reference, in order to estimate the increase in the pressure drop due to the presence of an obstruction in the flow.

The uniformity index was used to verify the distribution of microalgae along the photobioreactor length. It is defined as (Terashima *et al.*, 2009):

$$\mathrm{UI} = \frac{\sum_i |\alpha_{s,i} - \bar{\alpha}_s| V_i}{\bar{\alpha}_s V} \tag{12}$$

where V corresponds to the volume of the numerical cell, α is the microalgae volume fraction, and $\bar{\alpha}$ refers to the average value.

The swirl number was also evaluated. It is defined as (Gómez-Pérez *et al.*, 2017):

$$\mathrm{N_s} = \frac{\sum_i \mathbf{U_x} \mathbf{U}_\theta r A_i}{\sum_i \mathbf{U_x}^2 r A_i} \tag{13}$$

where r is the radial position, $\mathbf{U_x}$ is the axial component of the velocity, and $\mathbf{U}_\theta$ is the tangential velocity.

In addition the turbulent kinetic energy and the shear stress were used to evaluate the suitability of the flow to the bioprocess (Koerich and Rosa, 2017). Distribution fields were collected, as well as average values along the photobioreactor length.

3. RESULTS AND DISCUSSION

The GCI method was used to estimate the uncertainty of the results due to the mesh refinement. The results used for this analysis were the velocity of the liquid phase and the microalgae volume fraction, both collected in 10 points distributed along a vertical line at the outlet. According to the GCI method, the refined mesh (which had 135040 hexahedral control volumes) provided uncertainties of 1.02% and 0.34% for the prediction of velocity and volume fraction, respectively. The intermediate mesh (58500 control volumes) has uncertainties of 1.86% and 0.60% for velocity and volume fraction, respectively. Hence, the intermediate mesh was used to carry out the remaining simulations. For simulations considering reliefs, the intermediate mesh was subsequently refined and conformed to the internal surfaces, in a process that resulted in an even more refined mesh at the mixing region. On average, the chosen mesh provided y^+ values of 17.67.

Table 2 shows the pressure drop resulting from the flow in each evaluated case. It can be seen that the smooth tube provided the lowest pressure drop, which was expected, since there is no obstruction to the flow in this case. The inclusion of a horizontal bar in the tube resulted in an increase of 227.22 Pa, compared to the flow in a smooth tube. This is due to the increased friction caused by the bar, which was placed in the middle of a cross section of the photobioreactor (Y=0), which otherwise would have the highest velocity values. The inclusion of a ring baffle, in which the reliefs are near the tube walls, increased the pressure drop in 287.27 Pa, which is a bit higher than the case with a horizontal bar. The highest increase in the pressure drop was observed in the flow with a helical mixer, which were intended to only redirect the flow, without obstructing it. However, in this case there is more superficial area shearing with the flow, which can explain the increased pressure drop.

Table 2. Pressure drop resulting from the flow with different photobioreactor configurations.

Case	Pressure drop [Pa]	Pressure drop increase [Pa]
Smooth tube	99084.89	–
Bar	99312.11	227.22
Ring baffle	99372.16	287.27
Helical mixer	99668.96	584.07

Figure 2 shows the velocity distributions in each of the evaluated cases, in a plane placed in the middle of the photobioreactor. The smooth tube (Fig. 2a) has the typical velocity distribution, with higher values at the center and small

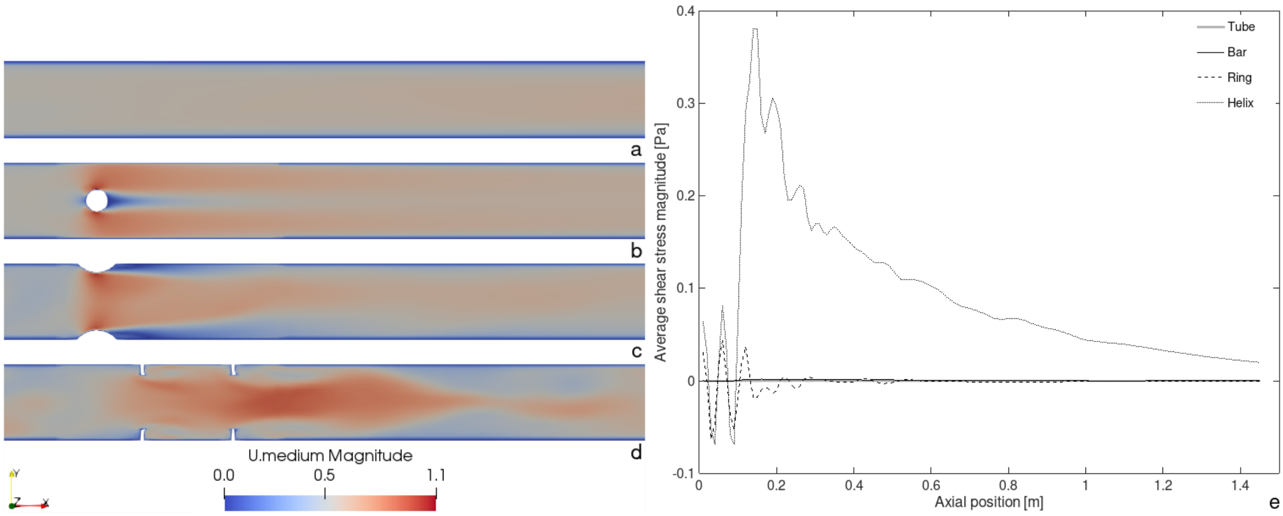

Figure 2. Velocity fields predicted for photobiorreactors with (a) smooth tube, and the inclusion of (b) a horizontal bar, (c) a ring, and (d) a helical mixer; (e) swirl number calculated along the length for each configuration.

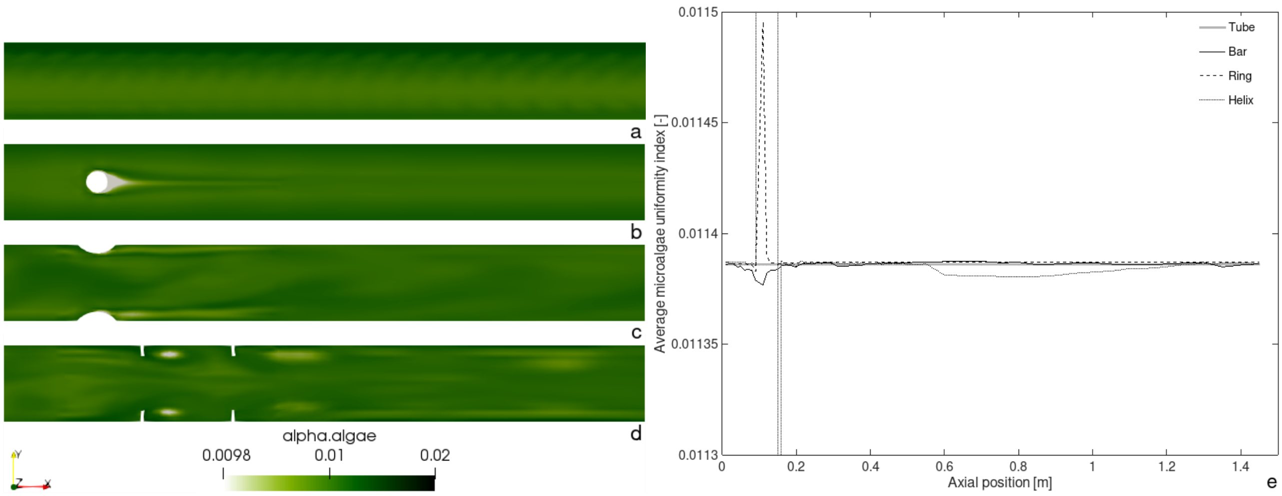

Figure 3. Microalgae volume fraction distribution predicted for photobiorreactors with (a) smooth tube, and the inclusion of (b) a horizontal bar, (c) ring baffle, and (d) a helical mixer; (e) uniformity index calculated along the length for each configuration.

velocities near the walls. Both the bar and the ring baffle (Figs. 2b and 2c) inserted in the photobioreactor cause an acceleration in the flow, near the obstruction surface. The helical mixer, promoted higher velocities near the axis of the tube (Fig. 2d). Figure 2e shows that the helical mixer enhanced significantly the swirl number of the flow, as expected. It reached a maximum value of $N_s \approx 0.4$, which is between "moderate" and "high" classification. High swirl numbers are beneficial for the culture mixing. However, this condition consumes much energy, and increases the shear stress (Gómez-Pérez *et al.*, 2017).

Figure 3a shows the phases distribution inside the smooth tube photobioreactor, in a plane placed in its middle. It can be noticed that the microalgae, which has a lower density compared to the liquid phase (Tab. 1) tends to accumulate near the top of the smooth tube. All obstructions inserted in the photobioreactor changed the phases distribution, promoting a mix between the phases to some extend. In general, Figs. 3b, 3c and 3d shows that the microalgae concentration decreases after the reliefs. This behavior had little effect on the uniformity index (Fig. 3e). In the smooth tube case, it is constant along the tube length, with a value of 0.011386. Regardless of the device used to promote mixture, the uniformity index reaches the same value few centimeters downstream. All predicted values were low, which indicates that the segregation that occurs in the photobioreactor is not an important problem considering the mixing between the phases. In spite of this, it is still interesting to have some kind of agitation in the photobioreactor to avoid plug-flow and to bring microalgae that are within the bulk of the flow to regions closer to the illuminated walls, hence enhancing the photosynthesis process.

Figure 4 shows the turbulent kinetic energy distribution predicted for each configuration. The inclusion of a horizontal bar (Fig. 4b) promoted a significant increase in the turbulent kinetic energy. Similarly, the inclusion of ring baffle around the tube wall also increased noticeably the turbulent kinetic energy (Fig. 4c). Both obstructions caused an acceleration

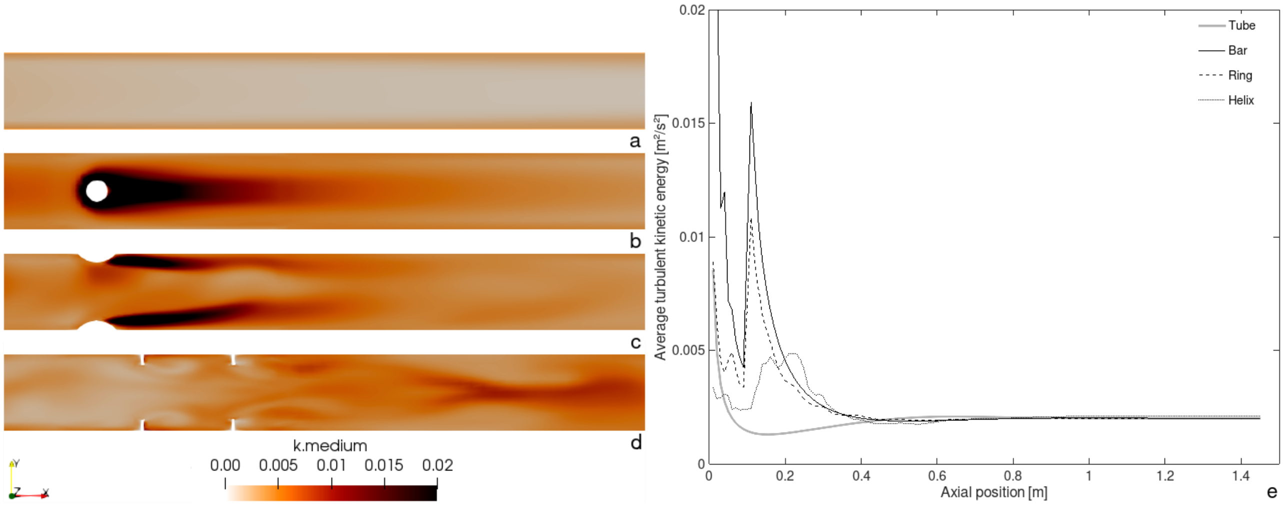

Figure 4. Turbulent kinetic energy predicted for photobiorreactors with (a) smooth tube, and the inclusion of (b) a horizontal bar, (c) ring baffle, and (d) a helical mixer; (e) average values calculated along the length for each configuration.

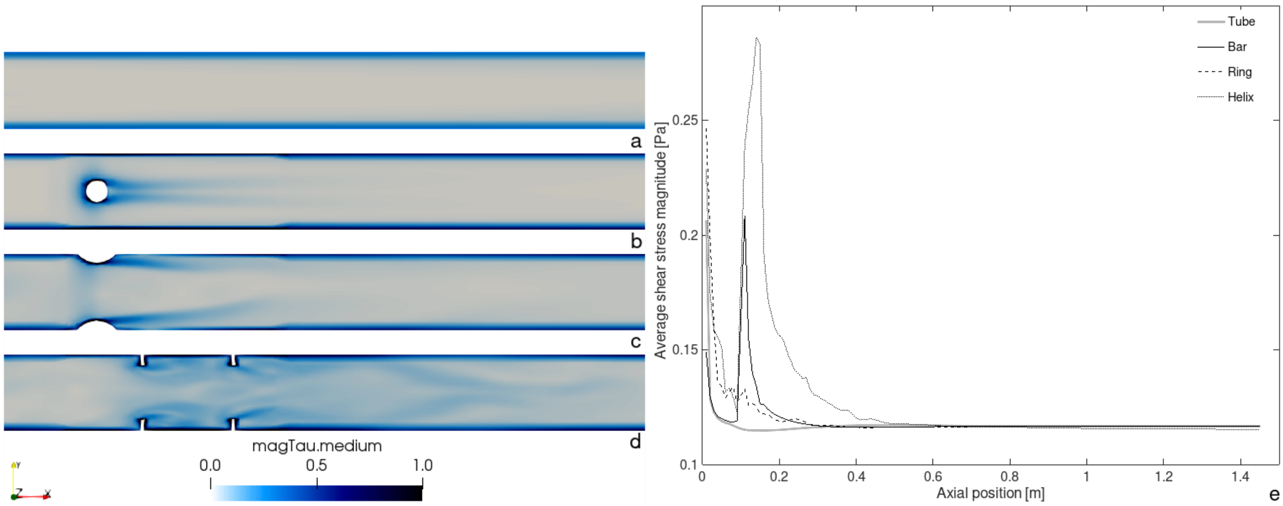

Figure 5. Shear stress predicted for photobiorreactors with (a) smooth tube, and the inclusion of (b) a horizontal bar, (c) ring baffle, and (d) a helical mixer; (e) average values calculated along the length for each configuration.

in the flow near the relief surface, resulting in higher shear rate and consequently higher turbulence production. The increased turbulence promotes higher microscopic mixing between microalgae and liquid medium. The helical mixer has as purpose to redirect the flow, increasing the tangential velocity. Hence, the turbulence promoted by this relief is smaller than those promoted by other cases. Figure 4e shows that the bar promoted the highest turbulence in the flow, followed by the ring baffle. Regardless of the case, the increased turbulent kinetic energy is dissipated along the tube length, being negligible after circa 0.5 m.

On the other hand, the higher superficial area of the helical mixer resulted in the highest values of shear stress (Fig. 5d). The inclusion of a horizontal bar and a ring baffle also increased the shear stress (Figs. 5b and 5c), in smaller magnitudes. The distribution of average values along the photobioreactor length is shown in (Fig. 5e). The insertion of an helical resulted in shear stress values higher than 0.2 Pa in the mixing region, which can be harmful to microalgae.

4. CONCLUSIONS

In this study, the effect of different obstacles on multiphase flow in a tubular photobioreactor was evaluated using the Computational Fluid Dynamics technique. The inclusion of obstacles promoted an increase in pressure drop, when compared to the flow inside a smooth tube. Microalgae tend to accumulate in the upper region of the photobioreactor, since their density is lower than the liquid medium. The inclusion of obstacles affects the distribution of microalgae, but did not promote improvement when evaluating the uniformity index, under the conditions evaluated. In the presence of the helical mixer, the flow inside the photobioreactor reached values greater than the swirl number (N_s=0.4), when compared to the other cases. The turbulent kinetic energy and shear stress were the most affected properties of the flow.

The inclusion of a horizontal bar promoted the largest increase in turbulent kinetic energy, while the helical mixer resulted in a greater increase in shear stress, reaching values above 0.2 Pa, which can be harmful to microalgae.

5. REFERENCES

Gidaspow, D., Seo, Y. and Ettehadieh, B., 1983. "Hydrodynamics of fluidization: Experimental and theoretical bubble sizes in a two-dimensional bed with a jet". *Chemical Engineering Communications*, Vol. 22. doi: 10.1080/00986448308940060.

Gudin, C. and Chaumont, D., 1991. "Cell fragility—the key problem of microalgae mass production in closed photobioreactors". *Bioresource technology*, Vol. 38, No. 2-3, pp. 145–151.

Gómez-Pérez, C.A., Oviedo, J.J.E., Ruiz, L.C.M. and van Boxtel, A.J.B., 2017. "Twisted tubular photobioreactor fluid dynamics evaluation for energy consumption minimization". *Algal Research*, Vol. 27, pp. 65–72.

Koerich, D.M. and Rosa, L.M., 2017. "Optimization of bioreactor operating conditions using computational fluid dynamics techniques". *Canadian Journal of Chemical Engineering*, Vol. 95, pp. 199–204. doi:10.1002/cjce.22635.

Menter, F., 1994. "Two equation eddy-viscosity turbulence models for engineering applications". *AIAA Journal*, Vol. 32, pp. 1598–1605.

Mitsuhashi, S., Fujimoto, M., Muramatsu, H. and Tanishita, K., 1994. "Effect of simple shear flow on photosynthesis rate and morphology of micro algae". *Acta Astronautica*, Vol. 33, pp. 179–187.

Roache, P.J., 1997. "Quantification of uncertainty in computational fluid dynamics". *Annual review of fluid Mechanics*, Vol. 29, No. 1, pp. 123–160. doi:10.1146/annurev.fluid.29.1.123.

Rossbach, V., Utzig, J., Decker, R.K., Noriler, D. and Meier, H.F., 2016. "Numerical gas-solid flow analysis of ring-baffled risers". *Powder Technology*, Vol. 297, pp. 320–329.

Su, Z., Kang, R., Shi, S., Cong, W. and Cai, Z., 2010. "Study on the destabilization mixing in the flat plate photobioreactor by means of CFD". *Biomass and Bioenergy*, Vol. 34, pp. 1879–1884.

Terashima, M., Goel, R., Komatsu, K., Yasui, H., Takahashi, H., Li, Y. and Noike, T., 2009. "CFD simulation of mixing in anaerobic digesters". *Bioresource technology*, Vol. 100, No. 7, pp. 2228–2233.

Wilcox, D.C. *et al.*, 1998. *Turbulence modeling for CFD*, Vol. 2. DCW industries La Canada, CA.

Zhang, Q., Wu, X., Xue, S. and K. Liang, W.C., 2013. "Study of hydrodynamic characteristics in tubular photobioreactors". *Bioprocess and Biosystems Engineering*, Vol. 36, pp. 143–150. doi:10.1007/s00449-012-0769-2.

6. RESPONSIBILITY NOTICE

The authors are the only responsible for the printed material included in this paper.